The Journal of Chemical Physics

RESEARCH ARTICLE | MARCH 18 2026

Polyampholyte model of ion clusters: Double-layer interactions in the presence of dissociated simple salt

David Ribar ; Clifford E. Woodward; Jan Forsman

Check for updates

J. Chem. Phys. 164, 114904 (2026)
https://doi.org/10.1063/5.0313308

View Online
Export Citation

Articles You May Be Interested In

Molecular interactions of acids and salts with polyampholytes
J. Chem. Phys. (February 2024)

Conformational transitions of a weak polyampholyte
J. Chem. Phys. (October 2014)

Dynamics of a single polyampholyte chain
J. Chem. Phys. (December 2021)

03 April 2026 20:58:01

AIP Advances
Why Publish With Us?
21DAYS average time to 1st decision
OVER 4 MILLION views in the last year
INCLUSIVE scope
Learn More
AIP Publishing

AIP Publishing

The Journal of Chemical Physics ARTICLE pubs.aip.org/aip/jcp

Polyampholyte model of ion clusters: Double-layer interactions in the presence of dissociated simple salt

Cite as: J. Chem. Phys. 164, 114904 (2026); doi: 10.1063/5.0313308
Submitted: 21 November 2025 • Accepted: 2 March 2026 •
Published Online: 18 March 2026

View Online Export Citation CrossMark

David Ribar,[1] Clifford E. Woodward,[2] and Jan Forsman[1,a)]

AFFILIATIONS

[1] Computational Chemistry, Lund University, P.O. Box 124, S-221 00 Lund, Sweden
[2] School of Physical, Environmental and Mathematical Sciences University College, University of New South Wales, ADFA, Canberra, ACT 2600, Australia

[a)] Author to whom correspondence should be addressed: jan.forsman@compchem.lu.se

ABSTRACT

We explore interactions between equally charged surfaces in the presence of simple salt and either neutral or monovalently charged polyampholytes. We consider the possibility of using these charged polymers as crude models of ion clusters. The latter have been hypothesized to form in concentrated aqueous salt solutions and are possibly related to *anomalous underscreening*. This phenomenon usually manifests itself in unexpectedly strong and long-ranged effective forces at very high ionic strengths. If ion clusters are formed, they are expected to carry at most a weak net charge. Keeping this in mind, we investigate how polyampholyte chains mediate interactions between charged surfaces. A significant amount of simple salt is also present in most cases. We highlight that if the charges of the polyampholytes are unevenly distributed, there is a polarization response that, in turn, can generate very strong and long-ranged surface forces, even at rather high concentrations of simple salt. Aside from their possible relevance to ion clusters and underscreening phenomena, these results also suggest the possibility of tailoring synthetic polyampholytes in order to regulate colloidal stability.

© 2026 Author(s). All article content, except where otherwise noted, is licensed under a Creative Commons Attribution (CC BY) license (https://creativecommons.org/licenses/by/4.0/). https://doi.org/10.1063/5.0313308

03 April 2026 20:58:01

I. INTRODUCTION

Using simple salts to tune the stability of colloidal dispersions containing charged particles is a long-established and theoretically well-grounded process.[1–13] For aqueous systems with monovalent ions, mean-field theories provide reliable predictions at low and intermediate concentrations. A central outcome of such treatments is the Debye screening length, λ_D, which characterizes the effective range of electrostatic interactions in an ionic medium. Increasing the salt concentration enhances ionic screening, thereby reducing λ_D $(\sim 1/\sqrt{c})$.

Surprisingly, recent measurements using the Surface Force Apparatus (SFA) have revealed a non-monotonic trend: beyond a threshold concentration (typically near 1 M), the range of effective repulsion between charged surfaces *increases* with added salt.[14–17] Similar trends have been reported in studies of colloidal stability[18] and thin films,[19] although conflicting results also exist.[20] Despite numerous theoretical efforts to rationalize these observations,[21–32] the molecular origin of this anomalous behavior remains unresolved.

One proposed mechanism involves the formation of ionic clusters, which would alter the effective free ion population and lead to unexpectedly long-ranged interactions at high ionic strengths.[14,29,30,32–35] Experimental evidence supporting ion clustering at high concentrations has been reported in previous studies.[36–43]

In this work, we examine surface forces in aqueous environments containing (mainly) linear ionic clusters that crudely mimic the ionic aggregates that may form in reality. We use an implicit solvent representation, where water enters only through its dielectric constant ($\varepsilon_r = 78.3$) and where some of the ions are connected to form linear aggregates. These clusters either carry a univalent net charge or are overall neutral. A population of simple salt (at least 100 mM) is also included in the (model) solution, keeping in mind that even if ion clusters are formed, one would anticipate a

© Author(s) 2026

remaining fraction of dissociated ions. These systems are analyzed using classical polymer Density Functional Theory (cDFT). We demonstrate that such "clustered electrolytes" can generate remarkably strong repulsive forces between similarly charged surfaces at short and intermediate separations, especially if the polyampholytes have a heterogeneous charge distribution, allowing a strong polarization response.

II. MODEL AND THEORY

The cartoon in Fig. 1 illustrates our two main models, which contain monodisperse ion clusters plus simple salt.

They are presented as monovalent linear 11-mer polyampholytes, which we denote as an 11:11 salt, keeping in mind that this does *not* imply that the species are multivalent. Indeed, we will restrict our models to contain only monovalent or net neutral polyampholytes. The single charged monomers are connected by bonds with a fixed length, b, but with full rotational freedom. While we primarily use linear architectures for these polyampholytes, some comparisons with results from branched chain models are made in Appendix A. We find that, at least for alternating charge models, cDFT predictions with linear and branched chains agree almost quantitatively.

We shall consider polyampholytes with two different charge arrangements: *alternating* charges and *block* charges. Even degrees of polymerization give neutral polyampholytes, whereas odd degrees of polymerization lead to a monovalent polyampholyte salt. We use r to denote the degree of polymerization (the number of monomers per polyampholyte chain). It should be noted that the *block* charge model might be prone to folding or flocculation at low concentrations of simple salt in the bulk solution, without a charged surface stabilizing the polarized structures. However, these polymers are likely to be soluble at high ionic strengths.

Unless otherwise specifically stated, surface interactions will be evaluated for like-charged walls with a surface charge density of $\sigma_s = -0.014286e/\text{Å}^2$. This is close to the estimated values for mica in a salt solution,[44] which are used in SFA experiments. The calculations are performed using polymer-cDFT, which accounts for hard-sphere exclusion between particles and with a mean-field treatment of Coulomb interactions.

Non-bonded interactions between monomers are described by the pair potential $\phi_{ij}(r)$, defined as

$$\beta\phi_{ij}(r) = \begin{cases} \infty, & r \le d, \\ l_B \dfrac{\eta_i \eta_j}{r}, & r > d, \end{cases} \tag{1}$$

where $\beta = (k_B T)^{-1}$ is the inverse thermal energy, and d denotes the monomer diameter. The Bjerrum length is $l_B \approx 7.16$ Å, and η_i and η_j denote the valencies of monomers i and j ($|\eta| = 1$ throughout this work), respectively. We use $n_+(\mathbf{r})$ and $n_-(\mathbf{r})$ to denote the densities of positive and negative polyampholyte monomers, whereas $n_c(\mathbf{r})$ and $n_a(\mathbf{r})$ are the concentrations of dissociated cations and anions.

We consider a system consisting of two infinite, rigid, and planar surfaces separated by a distance h. Each surface carries a uniform charge density, and the surfaces are immersed in the model mixture, and the inter-surface distance, h, is varied. The system is described within the grand canonical ensemble, implying that the confined fluid remains in chemical equilibrium with a bulk reservoir of infinite extent. For each separation, the equilibrium (minimal) free energy is determined, and the resulting osmotic pressure is evaluated either by numerically differentiating the free energy or via the contact densities of monomers at the surfaces. All polymer configurations are included following Boltzmann weighting, assuming that density variations occur solely in the direction perpendicular to the walls.[45]

In a completely ideal bulk polymer solution, where the only constraints are the intramolecular bonds and no intermolecular interactions or external potentials are present, the free energy $\mathcal{F}_p^{(id)}$ for an r-mer can be written exactly as

$$\beta\mathcal{F}_p^{(id)} = \int N(\mathbf{R})(\ln[N(\mathbf{R})] - 1)d\mathbf{R} + \beta\int N(\mathbf{R})V_b(\mathbf{R})d\mathbf{R}, \tag{2}$$

where $\mathbf{R} = (\mathbf{r}_1, \ldots, \mathbf{r}_r)$ denotes a polymer configuration, and $N(\mathbf{R})$ is the distribution function such that $N(\mathbf{R})d\mathbf{R}$ gives the number of polymer molecules with configurations in the range $[\mathbf{R}, \mathbf{R} + d\mathbf{R}]$. The bond potential between adjacent monomers is denoted as $V_b(\mathbf{R})$. In this work, we assume bonds of fixed length, i.e.,

$$e^{-\beta V_b(\mathbf{R})} \propto \prod \delta(|\mathbf{r}_{i+1} - \mathbf{r}_i| - b), \tag{3}$$

where we recall that b is the bond length, and $\delta(x)$ is the Dirac delta function. For the simple 1:1 salt, the corresponding ideal free energy, F_s, naturally lacks the polymer components,

$$\beta\mathcal{F}_s^{(id)} = \sum_{k=\{c,a\}} \int n_k(\mathbf{r})(\ln[n_k(\mathbf{r})] - 1)d\mathbf{r}, \tag{4}$$

where we recall that $n_c(\mathbf{r})$ and $n_a(\mathbf{r})$ denote the simple salt cation and anion densities, respectively.

In order to avoid complicated indexing, we will limit our cDFT description to models of net monovalent polyampholyte chains. The simplification that ensues for net neutral polyampholytes should be

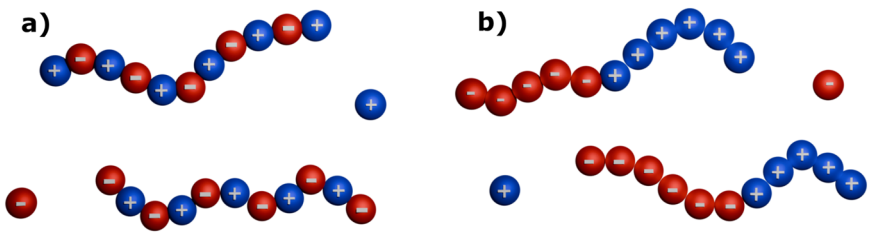


FIG. 1. An illustration of a (monovalent) 11:11 polyampholyte plus 1:1 simple salt. (a) The *alternating* charge model. (b) The *block* charge model.

03 April 2026 20:58:01

© Author(s) 2026

obvious. The Helmholtz free energy for the bulk polyampholyte salt model can be expressed as

$$\mathcal{F}(V,T,N_+,N_-,n_c,n_a) = \sum_{i=\pm}\mathcal{F}_{p,i}^{(id)} + \mathcal{F}_s^{(id)} + \mathcal{F}_{HS}^{(ex)}(n_+,n_-,n_c,n_a) + \mathcal{U}. \quad (5)$$

Here, i distinguishes between the two oppositely charged monovalent polymers, both being composed of an odd number of monomers. In bulk, both species contribute identically to the ideal free energy, while in confined or heterogeneous environments, their free energies differ. Excluded-volume effects are represented by $\mathcal{F}_{HS}^{(ex)}$, which depends on the total cationic and anionic monomer densities, n_+ and n_-, as well as the densities of the unconnected (simple salt) ions, n_c and n_a. This contribution is estimated using the Generalized Flory–Dimer (GFD) approach,[46] which accounts for differences in excluded volume between end monomers, dissociated monomers (simple salt ions), and inner monomers. All electrostatic terms are contained in $\mathcal{U}$ and are treated within the mean-field approximation.

In the slit geometry, with the planar charged surfaces separated by h, we employ the grand potential Ω, related to $\mathcal{F}$ by the Legendre transformation,

$$\begin{aligned}\Omega(V,T,\mu_p,\mu_s,\Psi_D;[N_+(\mathbf{Z}),N_-(\mathbf{Z}),n_c(z),n_a(z),\sigma_s])A^{-1} &= \mathcal{F}(V,T;[N_+(\mathbf{Z}),N_-(\mathbf{Z}),n_c(z),n_a(z),\sigma,V_{ex}(z,h)])A^{-1} \\ &- \int(\mu_p - e\Psi_D)N_+(\mathbf{Z})d\mathbf{Z} - \int(\mu_p + e\Psi_D)N_-(\mathbf{Z})d\mathbf{Z} \\ &- \int(\mu_c - e\Psi_D)n_c(z)dz - \int(\mu_a + e\Psi_D)n_a(z)dz, \end{aligned} \quad (6)$$

where e is the elementary charge, z denotes the coordinate perpendicular to the surfaces, $\mathbf{Z}$ is the planar generalization of $\mathbf{R}$, i.e., $\mathbf{Z} = z_1,\ldots,z_r$, A is the surface area, and Ψ_D is the Donnan potential that ensures overall electroneutrality. The total Helmholtz free energy $\mathcal{F}$ encompasses the contributions from configurational entropy, excluded-volume interactions, and mean-field electrostatics, including the wall–wall interaction. It is minimized for canonical equilibrium density distributions under the constraint of fixed numbers of polymers and simple ions, under the influence of the wall excluding potential $V_{ex}(z,h)$ and the surface charge density σ_s (at each wall). The grand potential Ω, on the other hand, is minimized for the equilibrium density distributions where the polymers and simple ions are in chemical equilibrium with a bulk distribution with fixed (input) polymer salt and simple salt chemical potentials, μ_p and μ_s. Note that one may view (say) $\mu_+^{eff} = \mu_p - e\Psi_D$ as an *effective* chemical potential of cationic polyampholytes (sometimes denoted as "electrochemical potential"), whereas $\mu_-^{eff} = \mu_p + e\Psi_D$. Analogous relations exist for the simple ions, of course. The surface interaction potential $V_{ex}(z,h)$ accounts for non-electrostatic exclusion and is purely steric, being zero within the accessible region $[d/2 < z < (h-d/2)]$ and infinite elsewhere. The equilibrium grand potential, $\Omega_{eq}(h)$, is obtained by numerical minimization using Picard iteration. Defining $g_s(h) \equiv \Omega_{eq}/A - p_b h$, where p_b is the bulk pressure, the net interaction free energy is given by $\Delta g_s \equiv g_s(h) - g_s(h\to\infty)$. In cases where the forces are quite long-ranged, the tail of this interaction is assumed to be an exponential decay (which is confirmed numerically below). We then set $g_s(h\to\infty) \approx g_s(h_0)$, where larger than 15 decay lengths (as estimated from the fit).

Further details of the numerical algorithm are available in Refs. 47 and 48, but a short summary is provided here. Due to planar symmetry and the mean-field approximation, densities and interactions can be integrated along the (x,y) directions parallel to the surfaces while maintaining electroneutrality. Accordingly, only z-dependent quantities are retained within the slit region. The laterally integrated Coulomb interaction between two monomers with valencies η_γ and η_δ at positions z and z' is given by $\beta\phi(z,z') = -2\pi\eta_\gamma\eta_\delta l_B|z-z'|$. We introduce $\lambda_{HS} \equiv \partial\mathcal{F}_{HS}^{(ex)}/\partial n_+ = \partial\mathcal{F}_{HS}^{(ex)}/\partial n_-$, noting that cationic and anionic monomers are of equal size.

Polymer configurations are treated within a classical density functional framework under mean-field weighting. The equilibrium monomer density is expressed in terms of auxiliary propagator functions $c(i,z)$, where i labels the monomer along the chain. Separate propagators, $c_+(i,z)$ and $c_-(i,z)$, are introduced for cationic and anionic chains, respectively. For cationic polymers, the contribution to the total monomer density $n'(z)$ at position z reads

$$n'(z) = e^{\beta\mu_+}\sum_{i=1}^{r} c_+(i,z)c_+(r+1-i,z), \quad (7)$$

where the prime indicates that only positively charged chains are considered. Propagator relationships will, of course, depend on the polymer architecture. For instance, if the chains have alternating charges, then the recursive relation governing the auxiliary functions is

$$c_+(i,z) = e^{\beta\lambda_{HS}(z)/2}\rho_+(z)^{(-1)^{(i-1)}}\int c_+(i-1,z') \times T(z,z')\rho_+(z')^{(-1)^i}dz' \quad (8)$$

for $i > 1$, and

$$c_+(1,z) = e^{\beta\lambda_{HS}(z)/2}\rho_+(z), \quad (9)$$

where $\rho_+(z) \equiv e^{-\beta e\Psi(z)/2}$ and $\Psi(z)$ is the local electrostatic potential (including Ψ_D). The kernel $T(z,z')$ imposes the fixed bond length constraint and includes a normalization factor,

$$T(z,z') = \frac{\Theta(|z-z'|-b)}{2b}. \quad (10)$$

Anionic chains are treated analogously, and for unconnected ions, there is no need for auxiliary functions, as there are no bond integrals.[48] To ensure stable convergence, conservative Picard iterations are applied, mixing a small fraction of updated densities with the previous ones, and the Donnan potential is simultaneously adjusted to maintain global electroneutrality. Convergence is achieved when the maximum relative change between successive iterations falls below 10^{-7} at all points.

In order to facilitate direct comparisons with SFA/AFM measurements, we will assume the validity of the Derjaguin approximation and present interaction free energies as force per radius, F/R.

03 April 2026 20:58:01

© Author(s) 2026

III. RESULTS. 1. NEUTRAL POLYAMPHOLYTES

We will initially explore surface interactions in the presence of net neutral polyampholytes, i.e., those composed of an even number of charged monomers.

A. Ideal dimers (zwitterions)

We begin by establishing the dipolar response of a fluid of ion pairs with opposite charges bonded at a distance b without hard cores. We denote these as "ideal dimers."

1. Dielectric response, no salt

We can evaluate the impact that these ideal dimers have on the overall dielectric response of the system[49] by calculating the net pressure between oppositely charged surfaces. In order to avoid saturation effects, which are likely to vanish in the presence of added salt anyway, we will, in this case, model these surfaces as weakly charged, $|\sigma_s| = 0.001e/\text{Å}^2$. Since there is no salt present, these oppositely charged walls will experience a constant attraction at long range, with a net pressure that is inversely proportional to the dielectric constant of the medium that separates them.

In the presence of zwitterions, this dielectric constant will shift from the reference value ε_w, in the absence of dipoles, to some higher value: ε. Hence, the ratio between these attractive pressures will directly give us the ratio $\varepsilon/\varepsilon_w$. The results for various zwitterion concentrations and charge separation values (b) are collected in Fig. 2(a). In agreement with experimental findings,[50,51] there is a linear dependence on concentration.

2. Ideal dimers and ideal salts

We now consider interactions between equally charged surfaces with a *standard* charge density of $\sigma_s = -0.014\,286e/\text{Å}^2$) in the presence of 1900 mM ideal dimers and 100 mM of a simple 1:1 (ideal) salt. These concentrations are commensurate with a salt solution that is overall 2 M, but in which a substantial degree of ion pairing occurs, leaving only 100 mM of dissociated salt. We note that, in this case, no charged species will carry a hard core. In Fig. 2(b), we see the effect of the zwitterions on the double layer repulsion, which is stronger when the zwitterions are present. This response is also affected by the bond-length of the dimers. From mean-field theory, we expect that the Debye length, λ_D, will scale as the square root of the dielectric constant, ε. Extracting the appropriate values from Fig. 2(a), we find $\varepsilon(b = 4\ \text{Å},\ 1900\ \text{mM})/\varepsilon_w \approx 1.55$ and $\varepsilon(b = 8\ \text{Å},\ 1900\ \text{mM})/\varepsilon_w \approx 3.20$. This implies that

$$\frac{\lambda_D(\text{b} = 4\text{Å}, 1900\ \text{mM})}{\lambda_D(\text{no dipoles})} \approx \sqrt{1.55} \approx 1.25 \tag{11}$$

and

$$\frac{\lambda_D(\text{b} = 8\text{Å}, 1900\ \text{mM})}{\lambda_D(\text{no dipoles})} \approx \sqrt{3.20} \approx 1.79. \tag{12}$$

These ratios can be directly compared with the observed electrostatic decay lengths, evaluated from inverted slopes of the logarithm of the net pressure, i.e., the dashed lines in Fig. 2(c). Denoting the inverse of these linearly fitted slopes by α, we obtain

$$\frac{\alpha(\text{no dipoles})}{\alpha(\text{b} = 4\text{Å}, 1900\ \text{mM})} \approx 1.26 \tag{13}$$

and

$$\frac{\alpha(\text{no dipoles})}{\alpha(\text{b} = 8\text{Å}, 1900\ \text{mM})} \approx 1.84. \tag{14}$$

Given the excellent agreement between these sets of values, we conclude that the increased double layer repulsion observed in the presence of the dimers can be fully ascribed to their dipolar response. This response, which obviously is quite strong, is often neglected in theoretical considerations of ion pairing and its impact on surface forces.

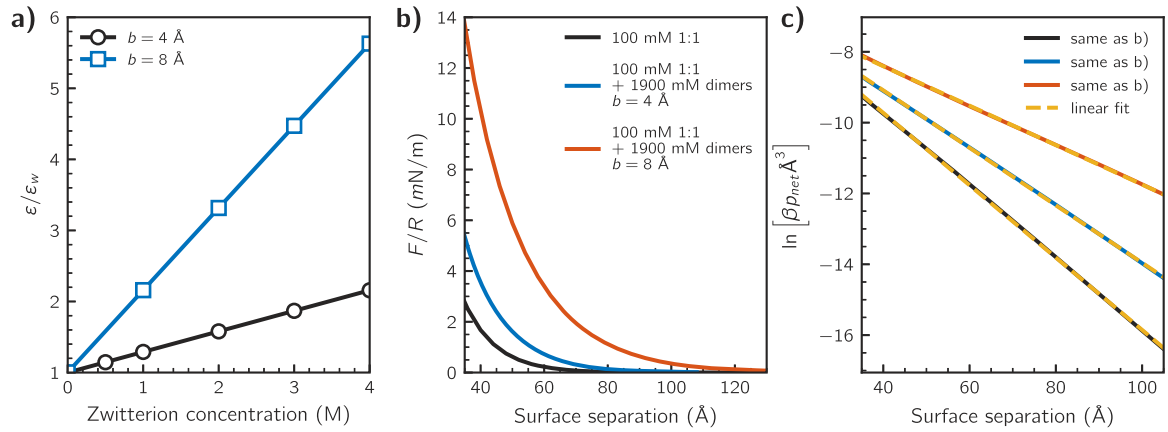


FIG. 2. (a) The dependence of $\varepsilon/\varepsilon_w$ on zwitterion concentration for two different choices of b. Calculated data are indicated by symbols. The lines are the linear regression fits. (b) Force per radius values between equally charged surfaces, in the presence of 1900 mM zwitterions and 100 mM simple 1:1 salt (no excluded volume). (c) The corresponding logarithm of the net pressure.

03 April 2026 20:58:01

© Author(s) 2026

B. Neutral polyampholytes plus simple salt. The "gradual growth" of neutral ion clusters

As stated earlier, the above solution can be viewed as a crude model wherein a 2 M 1:1 salt solution undergoes partial ion pairing, leaving 100 mM of dissociated salt. Let us now explore what happens if the clusters that are formed are larger. In particular, we will assume that r-mers are now formed from the 2 M 1:1 solution, with 100 mM free salt remaining. For instance, with $r = 10$, we will have a mixture of 100 mM 1:1 salt and 380 mM of neutral 10-mers. Furthermore, we will assume all species have hard cores of diameter $d = 4$ Å in our ongoing calculations. Connected monomers in the r-mers are separated by a bond-length of $b = 6$ Å.

1. Chains with alternating charges

In Fig. 3(a), we show the surface interaction free energies for systems with neutral r-mers containing *alternating* charges. As in the earlier case for ion pairs and simple salt, the presence of the neutral clusters leads to a significantly stronger repulsion when compared with the simple salt only solution. This is due to the enhanced dielectric response of the ionic chains. On the other hand, an increase of r from 10 to 20, even with a concomitant drop of the polymer concentration, has essentially no impact on the net surface interaction. This indicates the polarization response of the chains depends primarily on the number of bonded ions, rather than the concentration of the clusters.

2. Chains with block charge structure

The corresponding contribution from polyampholytes that are composed of two *blocks* of opposing charge is *enormous*. This is illustrated in Fig. 3(b). Such a complete charge separation is arguably an upper limit in "real" clusters, although one would expect a significant polarization response in the vicinity of the charged surfaces (a more realistic model, to be explored in future work). At this stage, we note that the double layer forces acting in these systems are quite sensitive to the internal structure of the polyampholytes, i.e., our model of ion clusters. In contrast to the case with *alternating* charges, we here see a strong dependence on polymer length, r. An increased degree of polymerization leads to a stronger *and* longer-ranged interaction when the chains have a *block* structure. This is not surprising, since the *block* architecture creates larger dipole moments due to

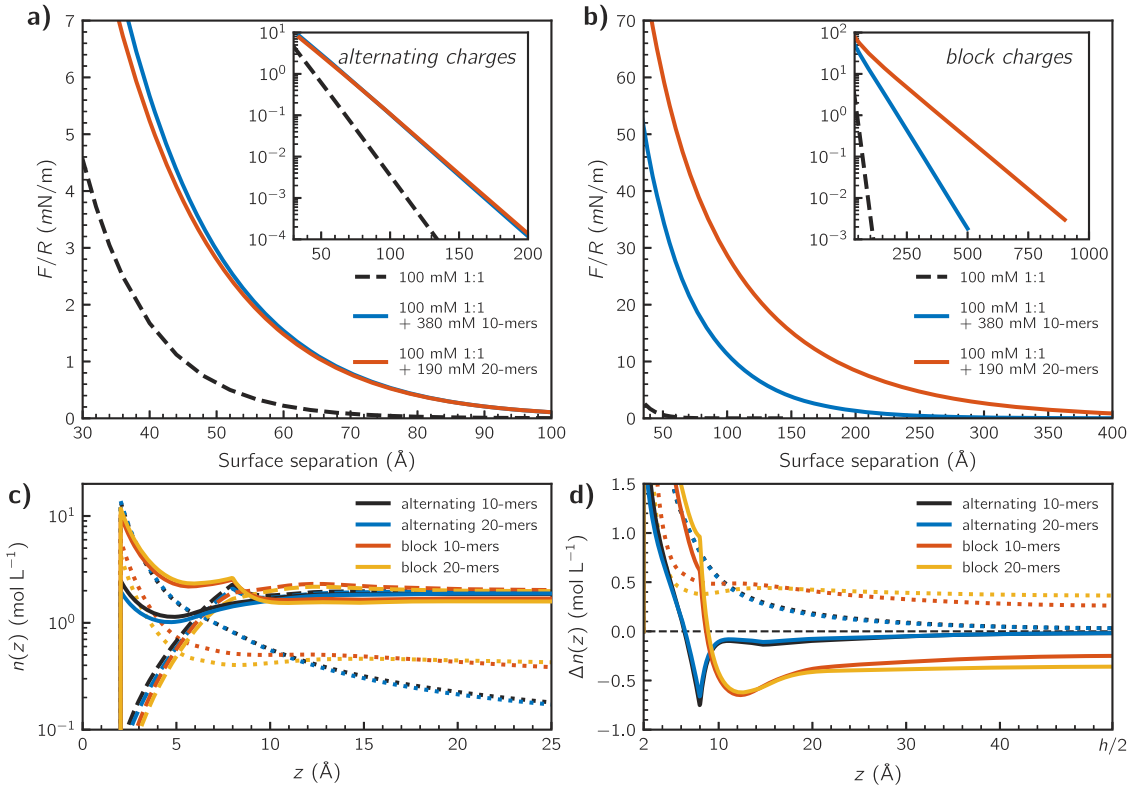


FIG. 3. Interactions between equally charged surfaces in the presence of neutral r-mer polyampholytes and 100 mM simple 1:1 salt (including excluded volume). For a given polymer length r, the polyampholyte concentration is chosen in a way that is commensurate with clustering of a 2 M simple salt solution. The case of a pure 100 mM simple salt solution is shown as a reference. The insert presents the logarithm of the F/R data. (a) The chains are composed of monomers with an *alternating* charge structure. (b) The chains are composed of monomers with a *block* charge structure. (c) Comparisons between density profiles of alternating and block charge structures. Full lines denote the polyampholyte n_+, dashed lines n_-, and dotted lines n_c. (d) Separate polymer and simple salt contributions to the net charge density, $\Delta n_p(z) \equiv n_+(z) - n_-(z)$ and $\Delta n_s(z) \equiv n_c(z) - n_a(z)$. Full lines denote the polyampholyte density differences, $\Delta n_p(z)$, while the dotted lines present the dissociated simple salt density differences, $\Delta n_s(z)$.

03 April 2026 20:58:01

© Author(s) 2026

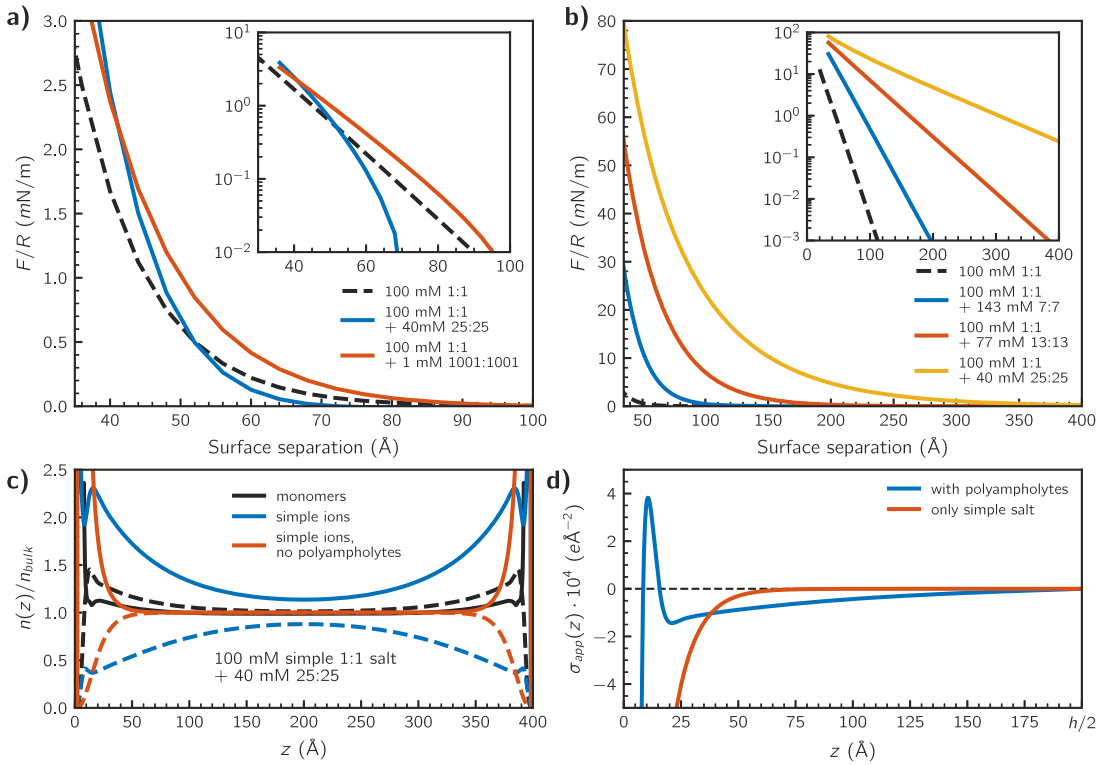


FIG. 4. (a) Surface forces in the presence of 100 mM pure 1:1 salt solutions, as well as in mixtures of 100 mM simple 1:1 plus added monovalent 25:25 (40 mM) or 1001:1001 (1 mM) salt. The concentrations of the polyampholyte salt are commensurate with an overall monomer concentration of 2000 mM. The *alternating* charge model has been adopted for the polyampholyte chains. (b) Surface forces in solutions similar to those in (a), but where the polymers have a *block* charge structure. (c) Density profiles, at $h = 400$ Å, in solutions containing 100 mM simple 1:1 salt and 40 mM 25:25 with a *block* charge architecture. Full lines denote the cations, while the dashed lines denote the anions. (d) Apparent surface charge density, $\sigma_{app}(z)$, for the system depicted in (c). The apparent surface charge density is defined as $\sigma_{app}(z) \equiv \sigma_s + \int_0^z \rho_c(z')dz'$, where $\rho_c(z)$ is the total charge density at position z.

an increased separation of larger charged blocks within each cluster. Both the separation and size of the charged blocks will increase approximately with the inverse of concentration. This means the dielectric response will also increase with the inverse concentration.

Monomer density profiles, as obtained with block and alternating chain architectures, are plotted in Fig. 3(c). We observe a relative enrichment of block monomers close to the charged surface that even exceeds the dissociated cation density at the surface (dotted lines). In Fig. 3(d), we present density differences, which correspond to separate contributions to the charge density profile. We see that for block structures, the charge density originating from polyampholytes is of comparable magnitude to that from the simple salt charge density, although with a different sign for $z > 8$ Å. That is to say, the polyampholyte monomer charge density is net negative in this distal regime, whereas the charge density originating from unconnected ions remains positive. This illustrates the origin of the expanded double layer established in the presence of block chains—cf. Fig. 4(c).

We have already mentioned that in a bulk solution, spontaneously formed ion clusters are unlikely to resemble *block* chains. Nevertheless, near a strongly charged surface, this is perhaps not a totally unrealistic description. Moreover, these predictions of surface forces with a truly remarkable range and strength, even with short polymer lengths, might imply novel applications of *synthesized* polyampholytes with a *block* charge structure.

Another property that might be relevant but is neglected in the current work is polydispersity effects. Real solutions of clustering ions will contain clusters of varying size, some of which are likely to be neutral, whereas others are weakly charged. Polydispersity effects are beyond the scope of the current study but will be investigated in future work.

IV. RESULTS. 2. MONOVALENT POLYAMPHOLYTES PLUS SIMPLE SALT

In a recent work,[52] we demonstrated that monovalent polyampholyte salts generate *much* stronger repulsive surface forces than a simple 1:1 salt at the same salt concentration. We have also established (above) how the presence of neutral "ion clusters," as modeled by our polyampholyte description, also leads to a substantially increased repulsion. Here, we will explore the surface force response to the presence of monovalent charged polyampholytes in addition to simple salt. We note that earlier simulation work has established that ion clusters tend to be either neutral or weakly

03 April 2026 20:58:01

© Author(s) 2026

charged.[29,32] This is also expected on physical grounds, since the formation of highly charged clusters would be associated with a considerable electrostatic free energy cost.

In Fig. 4(a), we see how the response to the addition of monovalent polyampholyte chains with an *alternating* charge is considerably weaker than when these are net neutral [cf. Fig. 3(a)]. Longer chains, at a constant monomer concentration, do increase the range somewhat, but the net increase of the repulsion is hardly dramatic.

On the other hand, when the polyampholytes have a *block* charge structure, they generate an *enormous* repulsion, even at high ionic strength and with relatively short chains. This is illustrated in Fig. 4(b), where we also note that the range *and* the strength of the surface interaction increase quite substantially when such polymers are added. As we have seen earlier, this is in turn related to a strong polarization of molecules with such an architecture.

The slow decay of the electrostatic potential, obtained in the presence of monovalent *block* charge polyampholytes, can also be illustrated by density profiles of charged species. In Fig. 4(c), we see how the polymer presence generates a remarkable extension to the thickness of the "diffuse" layer; i.e., the electrostatic potential decays much more slowly than in a corresponding salt solution without polyampholytes. A seemingly peculiar behavior is that the anionic monomers approach the midplane value from *above*, even though the surfaces carry a negative charge. The behavior arises from the combined effect of strong cooperative adsorption by the positive half (roughly) of the polymers and the molecular connectivity, which forces the rest of the chains to be located in rather close proximity, although in a broader region further away from the surface. We have tried to illustrate this further in graph (d) of Fig. 4, where we plot the "apparent" surface charge density, which, within a constant, is defined as the integrated total charge density outside the surface. Here, we note how the combination of effects discussed above leads to an apparent surface charge density that varies non-monotonically and with a rather long-ranged "tail" in a region distal to the surface.

A. Modeling the "gradual growth" of ion clusters with a *block* charge structure

Let us revisit a process similar to that we considered for neutral polyampholyte chains. We imagine a 2 M 1:1 salt solution in which monovalent *block* charge 25:25 clusters are formed to a gradually increasing extent. This then suggests a gradual drop of the remaining "free" ions, which together form a 1:1 salt. The corresponding cDFT predictions of surface forces are displayed in Fig. 5. As before, we find a dramatic impact from the presence of *block* polyampholytes. While we would expect that clusters of fully separated blocks of charge are unlikely, even at high ionic strength, the results may be viewed as a useful limiting case, at the opposite extreme to that of alternating charges. We would expect that alternating clusters should be preferred far from the charged surface, but the field from highly charged surfaces is expected to generate polarized (block-like) clusters in their vicinity. We expect that in a real scenario, surface forces will display a behavior between these two extremes.

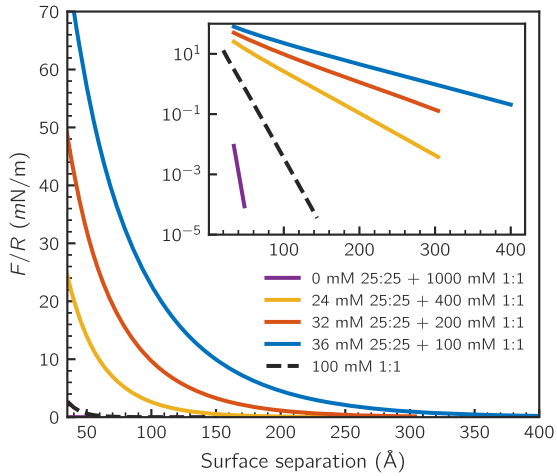


FIG. 5. Surface forces in the presence of pure 1:1 salt solutions and in mixtures of simple 1:1 and monovalent 25:25 salts. In the latter cases, the *block* charge model has been adopted. With one exception, the total concentration of positive, as well as negative, charged spheres in the bulk is 2 M. The case of a pure 100 mM simple salt solution is shown as a reference.

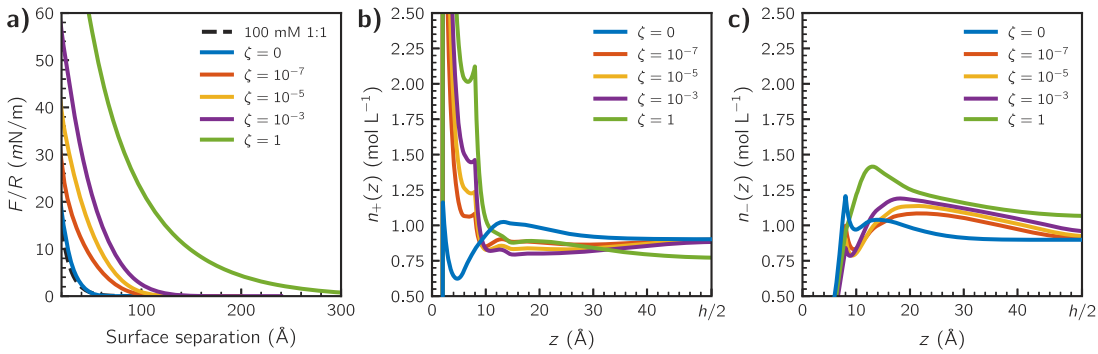


FIG. 6. A bulk solution composed of 100 mM simple 1:1 salt and mixtures of 36 mM monovalent 25:25 salt, a fraction ζ of which constitutes block charge chains, whereas the remainder $(1-\zeta)$ are polyampholytes with an alternating charge sequence. (a) Surface forces. (b) Cationic monomer density profiles. (c) Anionic monomer density profiles.

03 April 2026 20:58:01

© Author(s) 2026

B. Mixtures of monovalent polyampholytes plus simple salt

As we have already mentioned, it is possible that even though strongly polar clusters are rare in a bulk solution, they might be *formed* in the proximity of a charged surface. While we do not have the theoretical tools to describe such a chain architectural response, we can still estimate the relevance of such processes by allowing the presence of trace amounts of polar (block) chains in the bulk, which is dominated by polymers with an alternating sequence. In Fig. 6, we evaluate surface forces in mixtures of 100 mM simple 1:1 salt and 36 mM of monovalent 25:25 polyampholytes, of which a fraction ζ has a block charge structure, whereas the rest are composed of connected monomers with an alternating charge. We see how even a *tiny* amount of block polymers generates quite a strong repulsion. Note that $\zeta = 10^{-7}$ implies a chemical potential difference of more than $16k_BT$, suggesting that even if there is a high free energy cost to produce a polarized "cluster" in the bulk, these rare structures (in the bulk) can still have a strong impact on the surface forces. One should also note that typical polymer configurations are rather compact, i.e., the cartoon illustrations in Fig. 1 strongly exaggerate the degree of charge separation of typical polarized chains.

We obviously expect to recover the pure alternating chain results in the limit $\zeta \to 0$, but this is not obvious from the results presented in Fig. 6. This limit is reached at more reasonable fractions for a smaller degree of polymerization, and we have, therefore, included results obtained for 13-mers in Appendix B. The expected approach is clearly illustrated for such short chains, which also underlines the importance of cluster size in this respect.

V. CONCLUSIONS

We have demonstrated that a commonly adopted simplification, where ion cluster effects on surface forces are accounted for simply by the concomitant drop of the dissociated (free) ion concentration, may turn out to be inaccurate. This is because the ion clusters themselves contribute substantially to the interactions. Neutral clusters, modeled as chains of alternating charge (which may be prevalent due to the small Coulombic cost of creating them[29]), can have a significant effect due to their dielectric response. Moreover, the massive dipolar response we have observed for block architectures suggests that perhaps even a modest anisotropy of the ion cluster charge distribution may have a strong impact on the interaction between charged surfaces.

As already mentioned, our current models would benefit from the incorporation of polydispersity, as well as the ability of the chains to alter the connectivity in response to the presence of fields. These effects will be accounted for in future work, utilizing cDFT formulations that we have previously developed for similar systems.[53]

We have mainly discussed the polyampholytes as crude models of ion clusters, but it should be noted that our findings have broader implications. Given a solution of relatively high ionic strength, it would be quite feasible to *synthesize* polyampholytes with a *block* charge structure, for instance, using established biochemical approaches and suitably chosen peptides. Such *block* polyampholytes could then serve as stabilizers of colloidal dispersions, and their impact might be modulated by appropriate adjustments of pH. Moreover, the strong dipolar response that we observe is likely to be relevant in solutions containing "patchy" colloidal particles, such as proteins.

ACKNOWLEDGMENTS

J.F. acknowledges the financial support from the Swedish Research Council.

AUTHOR DECLARATIONS

Conflict of Interest

The authors have no conflicts to disclose.

Author Contributions

David Ribar: Conceptualization (equal); Formal analysis (equal); Validation (equal); Visualization (lead); Writing – original draft (supporting); Writing - review & editing (equal). **Clifford E. Woodward**: Conceptualization (equal); Methodology (equal); Writing – review & editing (equal). **Jan Forsman**: Conceptualization (equal); Formal analysis (equal); Funding acquisition (lead); Methodology (equal); Software (lead); Supervision (lead); Validation (equal); Writing – original draft (lead); Writing – review & editing (equal).

DATA AVAILABILITY

The data that support the findings of this study, as well as the code used to generate it, are freely available at the following Zenodo repository: https://doi.org/10.5281/zenodo.18466213.

APPENDIX A: BRANCHED POLYAMPHOLYTE STRUCTURES

1. Branched neutral chains (alternating charge)

It turns out that, at least within the mean-field approximation, there is no difference of practical importance between the multipole response from a linear or branched chain at a similar degree of polymerization. This is illustrated in Fig. 7(a).

This lends support to the hypothesis that a linear polymer model of ion clusters, which might appear unrealistically "stretched," actually is able to incorporate the most salient physics, at least for models of neutral polyampholytes with alternating charges. In other words, the overall multipole is quite similar (and significant) to models using branched polymer architectures.

2. Branched monovalent chains (alternating charge)

Here, we evaluate effects from making the charged monovalent polymer models more compact and, arguably, more cluster-like by using branched (star-like) backbone descriptions. As shown in Fig. 7(b), the branched chains mediate stronger but shorter-range surface forces. In the displayed case (40 mM monovalent 25-mers plus 10 mM 1:1 salt), the threshold separation is about 70 Å, below which the branched model produces a stronger repulsion.

03 April 2026 20:58:01

© Author(s) 2026

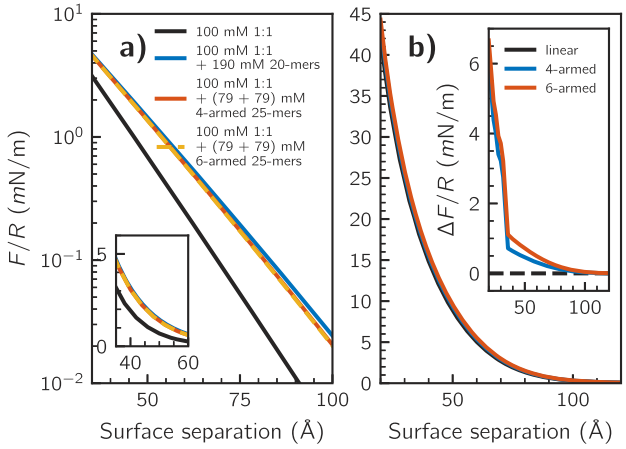


FIG. 7. (a) Interactions between equally charged surfaces in the presence of X mM r : r polyampholytes and 100 mM simple 1:1 salt. For a given degree of polymerization r, X is chosen in a way that is commensurate with the clustering of a 2 M simple salt solution. However, a neutral branched chain also contains an uncharged central monomer. Moreover, the branched chains form a mixture of polymers with cation/anion end charges (although all branches are overall electroneutral). This means that (say) a 25-mer cluster contains 24 charges and that there are two different versions of such a neutral cluster. (b) Surface forces, in the presence of a mixture of 10 mM simple 1:1 salt and 40 mM monovalent 25:25 salt (alternating charges). Apart from results for linear chains, we provide results for branched (star-like) 25-mer polyampholyte models with 4 and 6 "arms." The insert presents the difference between the linear surface forces to highlight the structure effect.

APPENDIX B: THE $\zeta \to 0$ LIMIT FOR POLYAMPHOLYTE MIXTURES WITH SIMPLE SALT

This part is added to illustrate that the interactions obtained from our simple salt + polyampholyte mixture do converge to the expected pure alternating chain (plus salt) limit as the fraction of block chains becomes vanishingly small, i.e., when $\zeta \to 0$. This is conveniently illustrated for polymers that are shorter than the 25-mers discussed in the main paper.

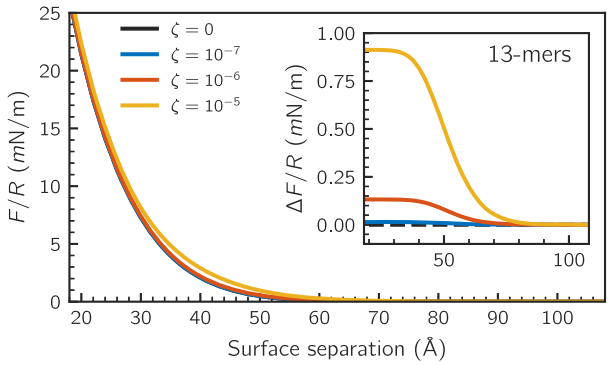


FIG. 8. A bulk solution composed of 100 mM simple 1:1 salt and mixtures of 69.2 mM monovalent 13:13 salt, a fraction ζ of which constitutes block charge chains, whereas the remainder $(1 - \zeta)$ are polyampholytes with an alternating charge sequence.

In Fig. 8, we note converged behaviors already for $\zeta \approx 10^{-7}$–10^{-6}. This is in contrast to our findings for 25-mers, highlighting the importance of cooperativity effects that are typical of polymeric systems. Our findings suggest that cluster polarization effects may dominate at even smaller fractions (or higher free energy costs per cluster) if the clusters contain more than 25 ions.

REFERENCES

[1] M. Gouy, J. Phys. Theor. Appl. **9**, 457 (1910).
[2] D. L. Chapman, "LI. A contribution to the theory of electrocapillarity," London, Edinburgh Dublin Philos. Mag. J. Sci. **25**, 475–481 (1913).
[3] B. V. Derjaguin and L. Landau, "Theory of the stability of strongly charged lyophobic sols and of the adhesion of strongly charged particles in solutions of electrolytes," Acta Phys. Chim. URSS **14**, 633–662 (1941).
[4] E. J. W. Verwey and J. T. G. Overbeek, *Theory of the Stability of Lyophobic Colloids* (Elsevier Publishing Company Inc., Amsterdam, 1948).
[5] F. Oosawa, *Polyelectrolytes* (Marcel Dekker, New York, 1971).
[6] L. Guldbrand, B. Jönsson, H. Wennerström, and P. Linse, "Electrical double layer forces, A Monte Carlo study," J. Chem. Phys. **80**, 2221 (1984).
[7] R. Kjellander and S. Marčelja, "Interaction of charged surfaces in electrolyte solutions," Chem. Phys. Lett. **127**, 402–407 (1986).
[8] S. Nordholm, "Generalized van der Waals theory. XII. Application to ionic solutions," Aust. J. Chem. **37**, 1 (1984).
[9] S. Nordholm, Chem. Phys. Lett. **105**, 302 (1984).
[10] J. N. Israelachvili, *Intermolecular and Surface Forces*, 2nd ed. (Academic Press, London, 1991).
[11] F. A. Evans and H. Wennerström, *The Colloidal Domain: Where Physics, Chemistry, Biology and Technology Meet* (VCH Publishers, New York, 1994).
[12] C. Holm, P. Kekicheff, and R. Podgornik, *Electrostatic Effects in Soft Matter and Biophysics* (Kluwer Academic Publishers, Dordrecht, 2001).
[13] J. Forsman, "A simple correlation-corrected Poisson–Boltzmann theory," J. Phys. Chem. B **108**, 9236 (2004).
[14] M. A. Gebbie, M. Valtiner, X. Banquy, E. T. Fox, W. A. Henderson, and J. N. Israelachvili, "Ionic liquids behave as dilute electrolyte solutions," Proc. Natl. Acad. Sci. U. S. A. **110**, 9674–9679 (2013).
[15] M. A. Gebbie, H. A. Dobbs, M. Valtiner, and J. N. Israelachvili, "Long-range electrostatic screening in ionic liquids," Proc. Natl. Acad. Sci. U. S. A. **112**, 7432–7437 (2015).
[16] A. M. Smith, A. A. Lee, and S. Perkin, "The electrostatic screening length in concentrated electrolytes increases with concentration," J. Phys. Chem. Lett. **7**, 2157–2163 (2016).
[17] Y. K. C. Fung and S. Perkin, "Structure and anomalous underscreening in ethylammonium nitrate solutions confined between two mica surfaces," Faraday Discuss. **246**, 370–386 (2023).
[18] H. Yuan, W. Deng, X. Zhu, G. Liu, and V. S. J. Craig, "Colloidal systems in concentrated electrolyte solutions exhibit re-entrant long-range electrostatic interactions due to underscreening," Langmuir **38**, 6164–6173 (2022).
[19] P. Gaddam and W. Ducker, "Electrostatic screening length in concentrated salt solutions," Langmuir **35**, 5719–5727 (2019).
[20] S. Kumar, P. Cats, M. B. Alotaibi, S. C. Ayirala, A. A. Yousef, R. van Roij, I. Siretanu, and F. Mugele, "Absence of anomalous underscreening in highly concentrated aqueous electrolytes confined between smooth silica surfaces," J. Colloid Interface Sci. **622**, 819–827 (2022).
[21] A. A. Lee, C. S. Perez-Martinez, A. M. Smith, and S. Perkin, "Scaling analysis of the screening length in concentrated electrolytes," Phys. Rev. Lett. **119**, 026002 (2017).
[22] F. Coupette, A. A. Lee, and A. Härtel, "Screening lengths in ionic fluids," Phys. Rev. Lett. **121**, 075501 (2018).
[23] B. Rotenberg, O. Bernard, and J.-P. Hansen, "Underscreening in ionic liquids: A first principles analysis," J. Phys.: Condens. Matter **30**, 054005 (2018).
[24] R. Kjellander, "A multiple decay-length extension of the Debye–Hückel theory: To achieve high accuracy also for concentrated solutions and explain

03 April 2026 20:58:01

© Author(s) 2026

under-screening in dilute symmetric electrolytes," Phys. Chem. Chem. Phys. **22**, 23952–23985 (2020).
[25]S. W. Coles, C. Park, R. Nikam, M. Kanduc, J. Dzubiella, and B. Rotenberg, "Correlation length in concentrated electrolytes: Insights from all-atom molecular dynamics simulations," J. Phys. Chem. B **124**, 1778–1786 (2020).
[26]J. Zeman, S. Kondrat, and C. Holm, "Bulk ionic screening lengths from extremely large-scale molecular dynamics simulations," Chem. Commun. **56**, 15635–15638 (2020).
[27]P. Cats, R. Evans, A. Härtel, and R. van Roij, "Primitive model electrolytes in the near and far field: Decay lengths from DFT and simulations," J. Chem. Phys. **154**, 124504 (2021).
[28]E. Krucker-Velasquez and J. W. Swan, "Underscreening and hidden ion structures in large scale simulations of concentrated electrolytes," J. Chem. Phys. **155**, 134903 (2021).
[29]A. Härtel, M. Bültmann, and F. Coupette, "Anomalous underscreening in the restricted primitive model," Phys. Rev. Lett. **130**, 108202 (2023).
[30]G. R. Elliott, K. P. Gregory, H. Robertson, V. S. J. Craig, G. B. Webber, E. J. Wanless, and A. J. Page, "The known-unknowns of anomalous underscreening in concentrated electrolytes," Chem. Phys. Lett. **843**, 141190 (2024).
[31]J. Forsman, D. Ribar, and C. E. Woodward, "An efficient method to establish electrostatic screening lengths of restricted primitive model electrolytes," Phys. Chem. Chem. Phys. **26**, 19921 (2024).
[32]D. Ribar, C. E. Woodward, and J. Forsman, "Solvent-induced ion clusters generate long-ranged double-layer forces at high ionic strengths," Soft Matter **21**, 5562–5572 (2025).
[33]K. Ma, J. Forsman, and C. E. Woodward, "Influence of ion pairing in ionic liquids on electrical double layer structures and surface force using classical density functional approach," J. Chem. Phys. **142**, 174704 (2015).
[34]K. Komori and T. Terao, "Cluster-size distribution of ions in concentrated aqueous NaCl solutions: Molecular dynamics simulations," Chem. Phys. Lett. **825**, 140627 (2023).
[35]D. Ribar, C. E. Woodward, S. Nordholm, and J. Forsman, "Cluster formation induced by local dielectric saturation in restricted primitive model electrolytes," J. Phys. Chem. Lett. **15**, 8326–8333 (2024).
[36]M. Sedlák, "Large-scale supramolecular structure in solutions of low molar mass compounds and mixtures of liquids: I. Light scattering characterization," J. Phys. Chem. B **110**, 4329–4338 (2006).
[37]M. Sedlák, "Large-scale supramolecular structure in solutions of low molar mass compounds and mixtures of liquids: II. Kinetics of the formation and long-time stability," J. Phys. Chem. B **110**, 4339–4345 (2006).
[38]Z. Liao, A. Das, B. Russell, I. Ahmed, I. Abate, I. MacLaren, R. Beveridge, and K. Wynne, "A metastable phase of amorphous aggregates governs solution structure," chemRxiv:2025-x4kh4/v2 (2026).
[39]D. J. M. Irving, M. E. Light, M. P. Rhodes, T. Threlfall, and T. F. Headen, "A total scattering study of prenucleation structures in saturated aqueous magnesium sulfate—Observation of extended clusters," Phys. Chem. Chem. Phys. **25**, 14898–14906 (2023).
[40]Y. Georgalis, A. M. Kierzek, and W. Saenger, "Cluster formation in aqueous electrolyte solutions observed by dynamic light scattering," J. Phys. Chem. B **104**, 3405–3406 (2000).
[41]E. O. Fetisov, C. J. Mundy, G. K. Schenter, C. J. Benmore, J. L. Fulton, and S. M. Kathmann, "Nanometer-scale correlations in aqueous salt solutions," J. Phys. Chem. Lett. **11**, 2598–2604 (2020).
[42]A. Shalit, S. Ahmed, J. Savolainen, and P. Hamm, "Terahertz echoes reveal the inhomogeneity of aqueous salt solutions," Nat. Chem. **9**, 273–278 (2016).
[43]J. S. Straub, M. S. Nowotarski, J. Lu, T. Sheth, S. Jiao, M. P. A. Fisher, M. S. Shell, M. E. Helgeson, A. Jerschow, and S. Han, "Phosphates form spectroscopically dark state assemblies in common aqueous solutions," Proc. Natl. Acad. Sci. U. S. A. **120**, e2206765120 (2022).
[44]A. R. Crothers, C. Li, and C. J. Radke, "A grahame triple-layer model unifies mica monovalent ion exchange, zeta potential, and surface forces," Adv. Colloid Interface Sci. **288**, 102335 (2021).
[45]C. E. Woodward, "Density functional theory for inhomogeneous polymer solutions," J. Chem. Phys. **94**, 3183 (1991).
[46]J. M. Wichert, H. S. Gulati, and C. K. Hall, "Binary hard chain mixtures I. Generalized flory equations of state," J. Chem. Phys. **105**, 7669 (1996).
[47]J. Forsman and C. E. Woodward, "Surface forces at restricted equilibrium, in solutions containing finite or infinite semi-flexible polymers," Macromolecules **40**, 8396 (2007).
[48]S. Nordholm, J. Forsman, C. Woodward, B. Freasier, and Z. Abbas, *Generalized Van Der Waals Theory of Molecular Fluids in Bulk and at Surfaces* (Elsevier, Amsterdam, 2018).
[49]Recall that the implicit solvent imposes a uniform dielectric constant ε_w.
[50]J. T. Edsall and J. Wyman, Jr., "Studies in the physical chemistry of betaines and related substances. I. Studies of dielectric constants and apparent molal volume1," J. Am. Chem. Soc. **57**, 1964–1975 (1935).
[51]R. Govrin, S. Tcherner, T. Obstbaum, and U. Sivan, "Zwitterionic osmolytes resurrect electrostatic interactions screened by salt," J. Am. Chem. Soc. **140**, 14206–14210 (2018).
[52]D. Ribar, C. E. Woodward, and J. Forsman, "Exceptionally strong double-layer barriers generated by polyampholyte salt," J. Phys. Chem. B **129**, 4241–4248 (2025).
[53]C. E. Woodward and J. Forsman, "Density functional theory for polymer fluids with molecular weight polydispersity," Phys. Rev. Lett. **100**, 098301 (2008).

03 April 2026 20:58:01

© Author(s) 2026